Dolomitization in the Lower Ordovician Watts Bight Formation of the St Georges Group, Western Newfoundland

James Conliffe[1], Karem Azmy, Ian Knight, and Denis Lavoie

J. Conliffe Department of Earth Sciences, Memorial University of Newfoundland, St. John's, NL, A1B 3X5, Canada, jamesconliffe@mun.ca

K. Azmy Department of Earth Sciences, Memorial University of Newfoundland, St. John's, NL, A1B 3X5, Canada, kazmy@mun.ca

I. Knight Geological Survey of Newfoundland and Labrador, Department of Natural Resources, Government of Newfoundland and Labrador, P.O. Box 8700, St. John's, NL, A1B 4J6, Canada.

D. Lavoie Geological Survey of Canada, GSC-Q, Natural Resources Canada, 490 de la Couronne, Québec, Qc, G1K 9A9, Canada.

[1] corresponding author (e-mail: jamesconliffe@mun.ca)

Abstract

The Watts Bight Formation in western Newfoundland consists of a succession of shallow water carbonates and has been extensively dolomitized. These dolomites occur as both replacements and cements and are associated with complex changes in the rock porosity and permeability. Early and pervasive replacement micritic dolomites (D1) are fine grained and indicate that dolomitisation began during early stages of diagenesis. The $\delta^{18}O$ of the earliest (D1) dolomitizing fluids (-6.4 to -8.4‰ VSMOW) fall between the estimated $\delta^{18}O$ values of the Tremadoc seawater and meteoric waters and suggest mixing-zone dolomitization. Later-stage replacement dolomites (D2) are associated with enhancement in porosity and permeability through the development of intercrystalline pores, while latest stage saddle dolomite (D3) and late burial calcite cements significantly occluded the pores in some horizons. Petrography, fluid inclusions and geochemistry show that D2 and D3 dolomites formed from warm (65 to 125°C) saline (10 to 25 eq. wt% NaCl + $CaCl_2$) hydrothermal fluids. The $\delta^{18}O_{fluid}$ of D2 ranges from -4.5 to 3.6 ‰ VSMOW and for D3 dolomites $\delta^{18}O_{fluid}$ ranges from 1.4 to 8.4 ‰ VSMOW, suggesting an influx of basinal brines. D2 dolomite crystals are often coated by a bituminous material which suggests either possible hydrocarbon charge after D2 dolomitisation or some local forced thermal maturation of organic matter.

The occurrence of high porosity associated with D2, combined with the laterally sealing tight limestone beds, presence of favourable source rocks and thermal maturation, may suggest that the Watts Bight carbonates are possible potential hydrocarbon reservoirs and suitable targets for future hydrocarbon exploration in Western Newfoundland.

1. Introduction

Hydrothermal dolomite (HTD) hydrocarbon reservoirs have been recognised as an important exploration target and are major hydrocarbon producers in North America (e.g., Davies and Smith 2006). This is because HTD reservoirs typically retain porosity and permeability much better than precursor limestones. Recently, dolostones including hydrothermal dolomites in the lower Paleozoic rocks of eastern Canada and the United States have been the focus of a number of studies (e.g., Cooper et al. 2001; Lavoie et al. 2005; Lavoie and Chi 2006; Smith 2006; Azmy et al. 2008). A number of factors point towards the hydrocarbon prospectivity of the Lower Ordovician St. George Group, Western Newfoundland, including the proximity of mature sources rocks (organic rich shales in the Green Point Formation) and impermeable cap rocks (Table Point Formation) and the successful drilling of the Port au Port #1 well in 1995 (Fowler et al. 1995; Cooper et al. 2001). In early 2007 extended testing from the reservoir in the upper part of the St. George Group, by Canadian Imperial Venture Corporation, resulted in the production of high API (50-56°) oil (315 barrels per day) and significant volume of natural gas (10^6 ft^3/ day).

The current study is focused on the Watts Bight Formation in the St. George Group, which is of particular interest for hydrocarbon exploration as it is extensively dolomitized and associated with significant porosity development (up to 30%; Cooper et al. 2001). The main objectives of this study are: (1) to identify and characterize (petrographically and geochemically) the dolomitization phases in the Watts Bight Formation; and (2) to investigate the origin and nature of the dolomitizing fluids of each phase to understand the diagenetic controls on porosity development and distribution. The results build upon

63 previously published data from the overlying Aguathuna and Boats Harbour Formations
64 (Azmy et al. 2008, in press) and will contribute to predictive models of the porosity
65 distribution in offshore and deeply buried onland counterparts

66 **2. Geological setting**

67 The Lower Paleozoic shelf rocks form part of the outer domain of the Humber zone in
68 Western Newfoundland, the westernmost of five tectono-stratigraphic zones in the
69 Canadian Appalachians (Fig. 1; Williams 1979). The evolution of these rocks during the
70 Lower Paleozoic has been discussed by several authors and summarized by Cooper et al.
71 (2001). Significant rifting, associated with the opening of the Iapetus Ocean, began
72 during the Late Proterozoic and Early Cambrian (Waldron and van Staal 2001; van Staal
73 2005) and is first recorded in Western Newfoundland by late Proterozoic, fault-bounded,
74 terrestrial clastics and volcanics of the lower Labrador Group. These deposits were
75 separated by a 90 million year hiatus from unconformably overlying clastic rocks of the
76 late Early Cambrian, upper Labrador Group (James et al. 1989). These mixed clastic-
77 carbonate sediments were overlain by a thick (1.5 km) Middle Cambrian to Lower
78 Ordovician carbonate platform succession, deposited on a passive margin to the south of
79 Laurentia. The Middle to Late Cambrian Port au Port Group is a narrow, high-energy
80 carbonate platform which evolved into a wide, low-energy carbonate platform
81 represented by the Early to Middle Ordovician St. George Group (James et al. 1989). A
82 regional unconformity, the St. George Unconformity, marks the top of the St. George
83 Group and a shift from a passive margin to a foreland basin (Knight et al. 1991). The St.
84 George Group is overlain by shelf carbonates of the Middle Ordovician Table Head
85 Formation (Stenzel et al. 1990), which were deposited in the foreland basin where they

86 are sporadically overlain by deep water carbonates and shales of the Table Cove
87 Formation (Stenzel et al. 1990).
88 The Ordovician St. George Group forms a sequence of subtidal and peritidal limestones
89 and dolostones and is widely exposed in western Newfoundland. The succession is
90 subdivided, in ascending order, into the Watts Bight, Boat Harbour, Catoche and
91 Aguathauna Formations (Fig. 2; Knight and James 1987) and represents at least two
92 sequences of Tremadoc and Arenigian age, termed megacycles by Knight and James
93 (1987). Each of these megacycles consists of a thin lower peritidal layer, a thick middle
94 subtidal layer and a thick upper peritidal layer (Knight and James 1987).
95 The Watts Bight Formation overlies the largely dolomitized peritidal carbonates of the
96 Upper Cambrian to Lower Ordovician Berry Head Formation of the Port au Port Group
97 (Knight et al. 2008) . It has been mapped throughout western Newfoundland (Knight and
98 James 1987) and is extensively dolomitized in many areas (Knight et al. 2008). On the
99 western shore of Isthmus Bay (Fig. 1), Port au Port Peninsula, a continuous ~69m section
100 of the formation (Fig. 2), described in detail by Knight et al. (2008), consists of two
101 sequences of low-energy bioturbated and mound carbonates overlain by higher energy
102 facies associations of mounds and grainstones. Knight et al. (2008) considered that these
103 sequences represented transgression and drowning of a shallow shelf, followed by
104 gradual accretion into the tidal zone.
105 At Isthmus Bay, dolomitization of the Watts Bight Formation is extensive particularly in
106 the lower and middle members where sucrosic dolostones replace both bioturbated and
107 thrombolitic limestone (Knight et al. 2008). These dolostones are dark-grey, fine to
108 medium grained and commonly have a strong condensate smell. Porosity is locally

developed in these dolostones, particularly is a section of dolomitized grainstones from the top of the middle member and in a thrombolitic dolostone ~12m above the base of the formation.

3. Methodology

The Isthmus Bay section was sampled approximately at intervals of ~ 2m (± 0.5m) and a total of forty three (43) samples were collected from the Watts Bight Formation. In addition, five samples were collected from the underlying Berry Head Formation of the Port au Port Group. Samples were analysed following the procedure outlined in detail by Azmy et al. (2008). In total 48 stained (Alizarin Red S-potassium ferricyanide; Dickson 1966) conventional thin sections were examined using transmitted light microscopy and cathodoluminescence (CL). Permeability was measured in selected dolomite samples using a computer controlled steady state permeameter (Temco Model MP-401).

Microthermometric fluid-inclusion analyses were performed using a Linkam THMSG600 heating-freezing stage. Calibration with precision of ± 0.2°C at –56.6°C and ± 1°C at 300°C was conducted using synthetic H_2O and CO_2 fluid inclusion standards. Salinities were calculated using a program by Chi and Ni (2006) for the system of H_2O-NaCl-$CaCl_2$ A polished mirror-image slab of each thin section was also prepared for microsampling. For C and O isotope analyses approximately 220µg of powder sample was reacted in an inert atmosphere with ultrapure concentrated (100%) orthophosphoric acid at 70°C in a Thermo Finnigan Gasbench II and the produced CO2 was automatically delivered to the source of a Thermo Finnegan DELTA V plus isotope ratio mass spectrometer in a stream of helium, where the gas was ionized and measured for isotope ratios. Precision of the data is better than ±0.1‰ for both $\delta^{18}O$ and $\delta^{13}C$ ratios. For major and trace element

analyses ~ 4mg of sample powder was digested in 2.5% (v/v) pure H_3PO_4 acid for 70-80 minutes and analysed for Ca, Mg, Sr, Fe and Mn (Coleman et al. 1989) using a HP4500plus inductively coupled plasma – mass spectrometer (ICP-MS). The relative uncertainties of these measurements are less than 5%.

Based on petrographic examination representative samples of dolomite were selected for Sr-isotope analysis at the at the Institut für Geologie, Mineralogie und Geophysik, Ruhr Universität, Bochum, Germany, following the procedures outlines in Azmy et al. (2008). The $^{87}Sr/^{86}Sr$ measurements were normalized to NBS 987 values bracketing the samples (0.710247) and corrected for deviation from value stated by McArthur (1994).

4. Results

4.1. Petrography

Based on petrography and CL, three distinct dolomitization events have been recognized. In addition, late-stage calcite diagenetic cementation phases and other diagenetic features (i.e. stylolites, sulphides and silicification) were described.

Micritic algae, limemud and early calcite cements

Micritic limemud (C1) was generally observed in limestone and dolomitic limestone samples. Limestones consist of peloidal and intraclastic micrite aggregates, with a micritic matrix or very fine-grained limemuds. Rarely skeletal grains (brachiopods and crinoids) are preserved, these are invariably replaced by coarser grained (100 to 300μm) anhedral Fe-poor calcite. In addition early calcite cement has been recorded in some of the interparticular pores (C2).

First dolomite

The first dolomite (D1) recognized in the samples is characterized by a fine-grained (< 25 to 50μm) crystals replacing C1 in dolomitic limestones (Fig. 3a). D1 commonly replaced sedimentary laminations and peloidal and intraclastic micrite aggregates and consists of tightly packed anhedral to subhedral rhombs with no visible intercrystalline porosity.

Second dolomite

A later phase of dolomites (D2) postdates D1, and comprises two sub-populations of dolomite replacement, designated D2a and D2b (Fig. 3b). D2a dolomite rhombs range in size from 40 to 150μm, are anhedral to subhedral and exhibit a dull luminescence under cathodoluminescence. Intercrystalline porosity in D2a is commonly low (<1%).

D2b dolomite is coarser grained than D2a (50 to 300μm) and rhombs are euhedral to subhedral with planar boundaries and an idiomorphic texture. D2b dolomite rhombs often show conspicuous zoning, with inclusion rich cores and inclusion poor rimes. D2b dolomite is associated with a significant increase in porosity (up to 7% intercrystalline porosity) and permeability (up to 16 md) although some of these pores are often filled by later diagenetic dolomite and calcite. Under CL, D2b dolomite displays a dull red luminescence, and commonly shows compositional zoning (Fig. 3e-f). When viewed under ultraviolet (UV) light, D2b rhombs showed yellow/dull luminescence zoning. D2a and D2b dolomite rhombs are also commonly coated by bituminous organic material.

Third dolomite

The latest void-filling dolomite (D3) occurs in previously uncemented pores and/or fractures. The D3 dolomite is relatively rare and consists of dolomite rhombs, which are euhedral to subhedral and range in size from 100 to 400μm. It usually displays undulose

extinction and commonly has non-planar boundaries, features typical of saddle dolomite (Warren, 2001). D3 dolomite displays a uniform red fluorescence under CL.

Other diagenetic features

D2 dolomite is both crosscut and bounded by high amplitude microstylolites, which postdate the early burial diagenesis. A translucent, coarse blocky calcite cement (C3) is common and fills pores and fractures still open after D3 precipitation (Fig. 3c). C3 calcite ranges in size from 50 to 400μm and both Fe-poor and Fe-rich calcite has been recorded. Under CL, it shows a uniform bright yellow luminescence. In addition rare pore-filling sphalerite and micro-quartz have been recorded.

4.2. Fluid inclusion analysis

Fluid inclusions were examined in D2 and D3 dolomite and C3 calcite and microthermometric data is summarized in Table 1. The fluid inclusions in dolomite (D2 and D3) were hosted in clusters in the core of dolomite crystals or in discrete zones within dolomite rhombs, and inclusions were commonly elongate in the direction of growth (Fig. 4a). Inclusions in C3 calcite were found in clusters in the core of crystals and can be very large with respect to their host crystals (up to 50μm; Fig. 4b). Therefore inclusions in dolomite and calcite are considered primary in origin and represent samples of fluid trapped during growth (Goldstein 2003).

D2 dolomite

Fluid inclusions in D2a and D2b dolomite are biphase and range in size from 2 to 20μm. Homogenization temperatures (T_h), representing the minimum estimates of entrapment temperatures, ranged from 44.6 to 108.6°C (average of 81.8°C ± 14.2°C; Figs. 5 and 6), with no significant variations recorded between inclusions hosted in the cores and rims of

D2b crystals. The initial melting temperatures (T_i) ranged from -55.2 to -51.3°C (Table 1), corresponding to the eutectic temperature for the H_2O-NaCl-$CaCl_2$±$MgCl_2$ system (Shepherd et al. 1985). Hydrohalite melting (T_m(hydrohalite)) occurred between -39.1°C and -31.9°C yielding X_{NaCl} values of between 0.14-0.28. Ice melting temperatures (T_m(ice)) ranged from -25 to -6.2°C, giving a wide range of fluid salinities (10.1 to 23.3 eq. wt% NaCl + $CaCl_2$; Fig. 6).

D3 dolomite

The fluid inclusions in D3 dolomite are biphase and range in size from 2 to 10µm. Inclusions homogenize (T_h) to the liquid phase between 91.4 and 130.1°C (114°C ± 13.3°C; Figs. 5 and 6). Initial ice melting temperatures (T_i) of -52 to -50.2°C indicate the presence of $CaCl_2$ ± $MgCl_2$. T_m(hydrohalite) of -31.5 to -30.2 was used to calculate X_{NaCl} of 0.29 to 0.34. T_m(ice) ranged from –14.7 to -21.3ºC, with calculated salinities from 17.8 to 21.7 eq. wt% NaCl + $CaCl_2$.

C3 calcite

Fluid inclusions in C3 calcite display a wide range of size (2 to 50µm) and degree of fill (0.6 to 0.95) and a large number of inclusions show evidence of post-entrapment leaking and/or stretching (e.g. microfractures at edge of inclusions: Fig. 4b). Care was taken only to record microthermometric data from inclusions which displayed small T_h variations within an individual inclusion group (e.g. a cluster), usually less than 10ºC, suggesting that post-entrapment effects are not important (Goldstein and Reynolds 1994). T_h values range from 68 to 126.7°C (average of 94.1 ± 17.3°C; Fig. 5). T_i ranged from -55.2 to -51°C (close to the eutectic temperature of the H_2O-NaCl-$CaCl_2$±$MgCl_2$). Hydrohalite melting occurred between -26.1°C and -34.6°C yielding X_{NaCl} values of between 0.22-

0.54. T_m(ice) occurred between -14.7 and -20.1°C corresponding to salinities ranging between 17.9 to 21 eq. wt% NaCl + $CaCl_2$.

4.3. Carbon and oxygen isotopes

The carbon and oxygen isotopic compositions of calcite and dolomite analysed are summarized in Figure 7 and Table 2. Because C1 and C2 were inseparable by conventional microdrilling, they are reported indistinctively and great care has to be taken in interpreting the data.

Calcites

Twelve analyses of C1/C2 calcite from the Watts Bight Formation yielded $\delta^{13}C$ values from -1.3 to -2.2‰ and $\delta^{18}O$ values of -7.4 to -8.4‰. The C3 cement was analysed from four samples and gave $\delta^{13}C$ values of -1.5 to -5.1‰ and $\delta^{18}O$ values of -7 to -8.5‰.

Dolomites

Two samples of D1 were collected from dolomitic limestones and gave $\delta^{13}C$ values of -1‰ and $\delta^{18}O$ values of -5.5 to -6.3‰. Fourteen D2a and twelve D2b dolomite samples yield very similar carbon and oxygen isotope values (Fig. 7, Table 2) with $\delta^{13}C$ values of -0.6 to -1.9‰ and $\delta^{18}O$ values of -5.5 to -11.4‰. Three analyses of D3 dolomite gave $\delta^{13}C$ and $\delta^{18}O$ values ranging from –1 to –2.1‰, and –5.6 to –9.6‰, respectively.

4.4. Strontium isotopes

A single sample of D1 dolomite yielded an $^{87}Sr/^{86}Sr$ ratio of 0.709283 ± 0.000007 (Fig 8; Appendix A). The range of $^{87}Sr/^{86}Sr$ for D2 dolomite is between 0.709106 ± 0.000007 and 0.708953 ± 0.000007 and the D3 dolomite yielded values (0.709075 ± 0.000007 to 0.7091 ± 0.000007) (Fig. 8; Appendix A).

4.5. Major and trace element geochemistry

The distribution of major and trace elements in calcite (C1/C2, C3) and dolomite (D1, D2, D3) from the Watts Bight Formation is summarized in Table 2. C1/C2 calcite is characterized by Sr concentrations of 319 ± 50ppm and low Mn and Fe values (168 ± 82ppm and 64 ± 23ppm, respectively). Dolomites from the Watts Bight Formation had Ca concentrations ranging from 64.1 to 54.2%. D1 dolomites had similar Sr contents to C1 (257ppm) but were relatively enriched in Fe (1323ppm) and Mn (96ppm). Compared to early diagenetic phases (C1/C2 and D1), Sr concentrations were significantly depleted (< 200ppm) in later dolomite and carbonate phases (D2a, D2b, D3, C3). Mn concentrations were relatively constant between D2a, D2b and D3 (63 ± 14ppm, 69 ± 20ppm and 59ppm respectively). .

5. Discussion

In the following section, petrographic and geochemical observations and data are presented in order to support our contention that hydrothermal fluids (e.g., fluids having temperature at least 5°C higher than ambient formation temperature; White 1957; Smith and Davies 2006) circulated in the Watts Bight Formation and are responsible for most of the dolomite observed in the unit.

5.1 Dolomite petrography

Dolomite 1 (D1) is fabric retentive dolomicrite, which commonly replaces early micrite and micritic peloids and intraclasts (C1) and it appears dull to non luminescent under luminoscope. It predates all other dolomite generations and stylolites and was most likely formed during the early diagenetic history prior to significant burial and compaction. Dolomite 2 (D2) includes 2 subphases, D2a and D2b, and is crosscut by and associated with microstylolites, which is consistent with dolomitization likely during shallow to

intermediate burial (e.g., Azmy et al., 2008). D2 dolomites are also often coated by a bituminous material which suggests that hydrocarbons migrated in pore space after D2 dolomitization.

Petrographic studies of the Watts Bight dolomites have shown that early diagenetic dolomitization (D1) led to a low porosity end-product (< 1%), whereas significant intercrystalline porosity (up to 7%) resulted from D2b dolomitization (Appendix A), as has been recorded from other successions in the St. George Group (Azmy et al. 2008, in press). This may indicate that early shallow dolomitization was extensive and occurred under open-system conditions with the circulation of a large volume of dolomite-saturated diagenetic fluids, so that no open pores were preserved. On the contrary, the higher intercrystalline porosity and non-stoichiometric nature of D2b dolomites is consistent with dolomitization of limestones under relatively closed-system conditions with a much lower fluid/rock ratio and a limited local supply of Mg^{2+} and CO_3^{2-} ions, as dolomite has a lower molar volume than calcite or aragonite (Warren 2000). The lower porosity associated with D2a dolomite may reflect the replacement of D1 dolomite, where no volume reduction would be expected.

A large number of intercrystalline pores in D2 dolomite have been occluded by D3 dolomite and C3 calcite (Fig. 4c, e, f), reducing the effective porosities of these early hydrothermal dolomites. However Knight et al. (2008) recognized two intervals at Isthmus Bay with increased intercrystalline and vuggy porosity. The upper porous interval is a dolomitized, crossbedded grainstone at the top of the middle member (porosity of 4 to 5%; Appendix A) and the lower porous interval is a thrombolitic boundstone dolomite ~12m above the base of the formation (porosity of ~7%; Appendix

A). Permeability measurements from selected dolomites (Appendix A) show that permeability in the upper porous interval is low (<2 mD) and is similar to permeability in other non-porous dolomites. However the lower porous interval is characterized by much higher permeability (10 to 16 mD), indicating a higher degree of interconnectivity between intercrystalline pores in D2b dolomite from this horizon. Cooper et al. (2001) reported similar high porosity and high permeability horizons associated with hydrothermal dolomites in the Watts Bight Formation from a series of exploration wells around Port au Port peninsula. Although there is no evidence that these porous horizons are laterally continuous this demonstrates that significant and preserved porosity can be associated with dolomites throughout the Watts Bight Formation.

5.2 Fluid inclusion data

There is an increase in the average homogenization temperature (T_h) of primary fluid inclusions from D2 dolomite (81.8 ± 14.2°C) to D3 dolomite (114 ± 13.3°C). This is consistent with an increase in burial depth during dolomitization and/or hydrothermal fluid influxes resulting in high temperature dolomitization. Maximum burial temperatures of 75°C have been estimated from conodont alteration indices (CAI), acritarch alteration indices (AAI) and graptolite reflectance data from the Lower Ordovician rocks of the Port au Port peninsula (Nowlan and Barnes 1987; Williams et al. 1998). Although the interpretation of this data is not straightforward (Williams et al. 1998) it suggests that most of the dolomitization in the Watts Bight Formation likely proceeded from fluids at temperature significantly higher than formation temperature at the time of alteration and, by commonly accepted definition, can be designated as hydrothermal. In the absence of local igneous intrusions, the most likely source of these hydrothermal fluids is from the

upwelling of basinal fluids from depth along extensional to transtensional faults and fractures (Davies and Smith 2006). Basin modelling of Cambrian and Ordovician successions in western Newfoundland have predicted that fault footwalls became the foci for dolomitizing fluids (Cooper et al. 2001) and this is similar to Ordovician hydrothermal dolomites elsewhere in eastern Canada (Lavoie et al. 2005; Lavoie and Chi in press) and the northeastern United States (Smith 2006). Fluid inclusions in C3 calcite are characterized by homogenization temperatures that are higher than maximum burial temperatures (94.1 ± 17.3) but lower than T_h from D3 dolomite, the late carbonate cementation is likely associated with slighter cooler hydrothermal fluid influxes after dolomitization of the Watts Bight Formation, possibly after a relative tectonic uplift.

Primary inclusions in D2 dolomite have a wide range of salinities (9.5 to 25.6 eq. wt% NaCl + $CaCl_2$; Fig. 6) over a narrow temperature range, indicative isothermal mixing between two end member fluids of contrasting salinities (Shepherd et al. 1985). The low salinity fluid may represent residual meteoric fluids, seawater or low salinity groundwater in interstitial pore space. The high salinity fluid most likely represents basinal brines which circulated through the basin along faults and fractures. In the absence of significant volume of evaporite deposits in the Cambrian and Ordovician rocks of western Newfoundland, the origin of these high salinity brines is largely unknown as is common in structurally-controlled hydrothermal dolomite (Davies and Smith 2006). No discernible relationship between T_h values and calculated salinities was recorded in D3 or C3 hosted inclusions.

5.3 Carbon and oxygen isotope data

The $\delta^{13}C$ data from C1/C2 calcite (Fig.7) show a narrow range of values (-0.3 to -2.2‰). These values are within the range of $\delta^{13}C$ values for the best preserved carbonates precipitated from Tremadoc seawater (0.0 to -2.5‰; Shields et al. 2003) and indicate that C1/C2 calcite preserves its Carbon isotope signature. Carbon isotope signatures from D1, D2 and D3 dolomite overlap those of C1 calcite (-0.6 to -2.1‰), reflecting the low CO_2 content of the dolomitizing waters in sedimentary basins (Land 1992), as such, the early to late dolomitization of the Watts Bight Formation occurred in a largely rock-buffered, closed diagenetic system.

The $\delta^{18}O$ of D1, D2 and D3 dolomites likely reflect the Oxygen isotopic composition of the dolomitizing fluids since dolomitization involves large volumes of waters to provide the Mg needed for the process. Therefore, the $\delta^{18}O$ of dolomites can be used to calculate the isotopic signature of the dolomitizing fluid ($\delta^{18}O_{fluid}$) and constrain the origin of these fluids. The $\delta^{18}O_{fluid}$ can be estimated using the equation of Land (1983), providing that the temperature of dolomitization can be obtained from the fluid inclusion homogenization temperatures. The dolomiciritic grain size and fabric retention of D1 suggest formation at near surface temperature (<50^{o}C) likely around 25°C (e.g., Budd, 1997; Warren, 2000; Azmy et al., 2001; 2008). Therefore, $\delta^{18}O_{D1}$ of -5.5 to -6.3‰ may suggest a parent fluid having $\delta^{18}O_{fluid}$ of -6.4 to -8.4‰ VSMOW (Vienna Standard Mean Ocean Water) (Fig. 9). The micritic lime mudstones and other depositional facies in the Watts Bight sediments indicate tropical shallow shelf water conditions. In similar present-day environments the $\delta^{18}O$ of seawater is ~ 0‰ and that of meteoric water is depleted by ~ 4‰ (Clark and Fritz 1997). The documented $\delta^{18}O$ of the best preserved primary calcite precipitated from the Tremadoc seawater during the deposition of the

Watts Bight carbonates is estimated at ~ -9.8‰ (Veizer et al. 1999; Shields et al. 2003), which translate to $\delta^{18}O_{seawater}$ of a warm (20 to 25°C) tropical zone of ~-6.3‰ VSMOW (Shields et al. 2003). Assuming that the relationship between the $\delta^{18}O$ of Tremadoc meteoric and seawaters were similar to those of our present day environment, the $\delta^{18}O$ of meteoric fluids were likely about -10.3‰ VSMOW. The calculated $\delta^{18}O$ values (-5.5 to -6.3‰ VSMOW) of the dolomitizing fluids of D1 (Fig. 9) seems to plot between the estimated $\delta^{18}O$ of the Tremadoc sea and meteoric waters (-6.3 and -10.3 ‰ VSMOW, respectively) and likely indicate a mixing zone model for early dolomitization as has been suggested for early dolomitization elsewhere in the St. George Group (e.g., Azmy et al., 2008, in press). This is also consistent with the low Sr contents in D1 (257 ppm) and the lack of evaporites deposits that do not support an evaporated brine origin as was believed by earlier studies (e.g., Lane, 1990).

Using the homogenization temperatures (estimates of minimum entrapment temperatures) recorded from primary fluid inclusions in D2 and D3 dolomites as proxies for temperature of dolomitization, the $\delta^{18}O_{fluid}$ has been calculated (Fig. 9). For D2 dolomite $\delta^{18}O_{fluid}$ ranges from -4.5 to 4.7 ‰ VSMOW and for D3 dolomites $\delta^{18}O_{fluid}$ range from 1.4 to 8.4 ‰ VSMOW. These values are much higher than would be expected from seawater or meteoric fluids and are consistent with dolomitization associated with an influx of basinal brines, which are commonly enriched in $\delta^{18}O$ (Goldstein and Reynolds 1994). The slightly lower $\delta^{18}O$ calculated for D2 dolomites may represent mixing of these brines with $\delta^{18}O$ depleted residual meteoric fluids as was suggested by the wide scatter of fluid inclusion salinity data.

5.4 Strontium isotope data

The $^{87}Sr/^{86}Sr$ value of the earliest D1 dolomite is close to that of early Ordovician (Tremadocian) seawater (Fig. 8; Shields et al. 2003). The Sr isotopic signature of replacive dolomite usually reflects the Sr isotopic signature of the precursor carbonate phase (Banner 1995) and this suggests that fabric retentive D1 dolomites preserve the primary signature of their precursor carbonates. The $^{87}Sr/^{86}Sr$ values are also supportive of a largely rock-buffered early dolomitization as suggested from $\delta^{13}C$ ratios. Our limited dataset of $^{87}Sr/^{86}Sr$ signatures for D2 and D3 dolomite indicate significant overlap with both D1 and the accepted value for Tremadocian seawater (Fig. 8). This indicates the lack of significant interaction between the dolomitizing fluid with any feldspar (Rubidium)-rich unit (crystalline basement or sandstone). This observation is again supportive of our contention of a largely rock-dominated diagenetic system with the ultimate source of the radiogenic strontium being Tremadocian limestones altered through circulation of the hydrothermal fluid. This scenario is consistent with previous studies of dolomitization in stratigraphically younger units of the St. George Group (Azmy et al. 2008, in press) but strongly differs from the more open diagenetic conditions recorded from the largely coeval Romaine Formation from nearby Anticosti Island (Lavoie et al. 2005; Lavoie and Chi, in press). .

5.5 Major and trace element geochemistry

The major element geochemistry of Watts Bight Formation dolomites (Appendix 1, Table 2) show that all dolomites (D1 to D3) are non-stoichiometric and Ca-rich (Ca concentrations range from 64.1 to 54.2%). No trends of increasing stoichiometry in hydrothermal dolomites from D2a (early) to D3 (late) has been observed, as would be expected for dolomites formed in open diagenetic systems and continuing dissolution and

405 re-precipitation (Sperber 1984; Montanez and Read 1992). Non-stoichiometric
406 dolomitization indicate formation in a relatively close and rock-buffered diagenetic
407 systems characterized by low volumes of fluid throughout (Sperber 1984; Kirmaci and
408 Akdag 2005).
409 With the exception of early D1 dolomite (Sr concentration = 257ppm), the Sr
410 concentration of later dolomites are low (101 ± 59ppm). These values are lower than
411 would be expected from dolomites associated with hypersaline waters (<550ppm; Tucker
412 and Wright 1990) and likely suggests that dolomitizing fluids were modified seawater
413 that circulated in the sedimentary basin. The relative higher Sr concentrations in D1
414 might be related to some contamination from precursor calcite that was very difficult to
415 avoid during microsampling since the Sr content is still within the low zone (257ppm),
416 suggesting that D1 originated from also modified seawater possibly in a mixing zone
417 environment (e.g., Azmy et al., 2008).
418 The iron and manganese content of dolomites may reflect, at times, the redox state of the
419 dolomitizing fluids since Fe and Mn are commonly enriched in the later diagenetic phases
420 (Tucker and Wright 1990). Hydrothermal dolomites (D2 to D3) in the Watts Bight
421 Formation have low Fe contents (< 1250ppm) when compared to hydrothermal dolomites
422 from elsewhere in the St. George Group (Azmy et al. 2008). In addition the general, but
423 statistically not significant, trend of decreasing Fe from D2a (early hydrothermal)
424 dolomite to D3 (late-stage) dolomite in the Watts Bight Formation (Table 2) is contrary
425 to what is normally seen during burial diagenesis (Tucker and Wright 1990) and may
426 reflect lower Fe and Mn concentrations due to lack of sources of these elements in the

surrounding rocks, particularly under closed system conditions of circulation, rather than variations in the redox state of the hydrothermal fluids.

5.6 Reservoir potential in the Watts Bight Formation

Hydrothermal dolomites and associated limestones have been demonstrated to be one of the most significant targets for hydrocarbon exploration in eastern North America (e.g. Lavoie et al. 2005; Smith 2006; Azmy et al. 2008). Hydrothermal dolomitization during early burial is an important process in the development of secondary porosity and permeability in potential hydrocarbon reservoirs (e.g. Smith 2006; Wierzbicki et al. 2006; Lavoie and Chi in press). Therefore, petrographic and geochemical investigations of diagenesis in these dolomites provide a better understanding of the timing and origin of diagenetic fluids, key controls on porosity evolution and distribution in potential reservoir rocks (Smith 2006; Wierzbicki et al. 2006).

This study demonstrates that the pore network and diagenetic evolution of the Watts Bight Formation recorded significant porosity development associated with the migration of hydrothermal fluids and hydrothermal dolomitization. In many locations in Western Newfoundland sucrosic dolomites (similar to D2) in the St. George Group are spatially associated with faults e.g. Daniels Harbour, Port au Choix (Knight et al. 2008). At Isthmus Bay the upper porous level is associated with a normal fault, now filled in with C3 calcite. Although no major faults have been reported from the lower porous level, hydrothermal fluids may have infiltrated along microfractures that have been recognised during petrographic analysis of Watts Bight dolomites. The exact timing of the hydrothermal dolomitization in western Newfoundland is unknown a Devonian age has been suggested by Cooper et al. (2001). This age is supported by Devonian Rb-Sr ages

from sphalerite in the Daniel's Harbour MVT deposit in western Newfoundland (Lane 1990) which provides an upper age limit for D2 and D3 dolomitization. Potential hydrocarbon charges postdate hydrothermal dolomitization as D2 rhombs are commonly coated by a bituminous material; the original hydrocarbons might have utilized the enhanced porosity and permeability of dolomite horizons in the Watts Bight Formation. Cooper et al. (2001) demonstrated that potential source rock in western Newfoundland entered the oil window in the Late Devonian, by which time extensional faulting would have juxtaposed the source rocks of the Green Point Formation and the dolomites of the St. George Group. Lateral and vertical variations in the porosity distribution in the Watts Bight Formation, due to the transition between porous hydrothermal dolomites and non-porous dolomites and limestones, would have facilitated the development of diagenetic traps and potential diagenetic reservoirs for hydrocarbon accumulations, as has been noted in other hydrothermal fields in eastern North America (e.g., Davies and Smith 2006; Wierzbicki et al. 2006).

6. Conclusions

Petrographic, fluid inclusion, stable isotope and trace element data indicate that there are at least three types of dolomite in the Watts Bight Formation, representing early diagenetic to late-stage hydrothermal dolomites. Early replacement micritic dolomites (D1) are fine grained and indicate that dolomitization began during the earliest stages of diagenesis. The $\delta^{18}O$ of D1 dolomitizing fluids (-6.4 to -8.4‰ VSMOW) fall between the estimated $\delta^{18}O$ of the Tremadoc sea and meteoric waters and support a mixing-zone dolomitization, as has been suggested elsewhere in the St. George Group.

Later-stage replacement dolomites (D2) are associated with enhancement in intercrystalline porosity and permeability through the development of intercrystalline pores, while latest stage saddle dolomite (D3) and late burial calcite cements, significantly occluded the pores in some horizons. The D2 dolomite crystals are often coated by a bituminous material which suggests possible hydrocarbon charge after D2 dolomitization. Fluid-inclusion microthermometric data imply that D2 and D3 dolomites were formed from warm, saline fluids of hydrothermal origin. The $\delta^{18}O_{fluid}$ of D2 ranges from -4.5 to 3.6 ‰ VSMOW and for D3 dolomites $\delta^{18}O_{fluid}$ ranges from 1.4 to 8.4 ‰ VSMOW, suggesting an influx of $\delta^{18}O$ heavier basinal brines.

The high porosity and permeability associated with D2 dolomites has been recorded in other cored sections from the Watts Bight Formation and combined with tight limestone beds, presence of favourable source rocks and thermal maturation, may suggest that the Watts Bight Formation carbonates are possible potential hydrocarbon reservoirs and suitable targets for future hydrocarbon exploration in Western Newfoundland.

Acknowledgements

This project was financed by the PPSC (Pan-Atlantic Petroleum Systems Consortium), and by ISPSG (Irish Shelf Petroleum Studies Group, Ireland). Support from the Earth Science Sector of Natural Resources Canada and by the Department of Natural Resources and Mines of Newfoundland and Labrador is warmly acknowledged. Nicolas Pinet is thanked for reviewing an early draft of this paper. This is Geological Survey of Canada contribution 20080544

493 **References**

494 Allan, J.R., and Wiggins, W.D. 1993. Dolomite reservoirs; geochemical techniques for
495 evaluating origin and distribution. AAPG Continuing Education Course Note
496 Series **36,** 129p.
497 Azmy, K., Lavoie, D., Knight, I., and Chi, G. 2008. Dolomitization of the Lower
498 Ordovician Aguathuna Formation carbonates, Port au Port Peninsula, western
499 Newfoundland, Canada: implications for a hydrocarbon reservoir. Canadian
500 Journal of Earth Sciences, **45**: 795-813.
501 Azmy, K,, Knight, I., Lavoie, D., and Chi, G., accepted. Origin of the Boat Harbour
502 dolomites of the St. George Group in western Newfoundland, Canada:
503 implications for porosity controls. Bulletin of Canadian Petroleum Geology.
504 Banner, J.L. 1995. Application of the trace element and isotope geochemistry of
505 strontium to studies of carbonate diagenesis. Sedimentology, **42**(5): 805-824.
506 Budd, D.A. 1997. Cenozoic dolomites of carbonate islands; their attributes and origin.
507 Earth-Science Reviews, **42**(1-2): 1-47.
508 Chi, G., and Ni, P. 2007. Equations for calculation of NaCl/(NaCl+$CaCl_2$) ratios and
509 salinities from hydrohalite-melting and ice-melting temperatures in the H_2O-
510 NaCl-$CaCl_2$ system. Acta Petrologica Sinica, **22**.
511 Clark, I.D., and Fritz, P. 1997. Environmental isotopes in hydrogeology. Lewis Publisher,
512 Boca Raton, Fla.
513 Coleman, M.L., Walsh, J.N., and Benmore, R.A. 1989. Determination of both chemical
514 and stable isotope composition in milligramme-size carbonate samples.
515 Sedimentary Geology, **65**(3-4): 233-238.
516 Cooper, M., Weissenberger, J., Knight, I., Hostad, D., Gillespie, D., Williams, H.,
517 Burden, E., Porter-Chaudhry, J., Rae, D., and Clark, E. 2001. Basin Evolution in
518 Western Newfoundland: New Insights from Hydrocarbon Exploration. AAPG
519 Bulletin, **85**(3): 393-418.
520 Davies, G.R., and Smith, L.B., Jr. 2006. Structurally controlled hydrothermal dolomite
521 reservoir facies: An overview. AAPG Bulletin, **90**(11): 1641-1690.
522 Dickson, J.A.D. 1966. Carbonate identification and genesis as revealed by staining.
523 Journal of Sedimentary Research, **36**(2): 491-505.
524 Fowler, M.G., Hamblin, A.P., Hawkins, D., Stasiuk, L.D., and Knight, I. 1995. Petroleum
525 geochemistry and hydrocarbon potential of Cambrian and Ordovician rocks of
526 western Newfoundland. Bulletin of Canadian Petroleum Geology, **43**(2): 187-213.
527 Goldstein, R.H., and Reynolds, T.J. 1994. Systematics of fluid inclusions in diagenetic
528 minerals. SEPM Short Course, Tulsa.
529 Goldstein, R.H. 2003. Petrographic analysis of fluid inclusions. *In* Mineralogical
530 Association of Canada, Short Course Series. *Edited by* I. Samson, A. Anderson,
531 and D. Marshall. pp. 9-53.
532 James, N.P., Stevens, R.K., Barnes, C.R., and Knight, I. 1989. Evolution of a lower
533 Paleozoic continental-margin carbonate platform, northern Canadian
534 Appalachians. Special Publication - Society of Economic Paleontologists and
535 Mineralogists, **44**: 123-146.
536 Kirmaci, M.Z., and Akdag, K. 2005. Origin of dolomite in the Late Cretaceous-Paleocene
537 limestone turbidites, eastern Pontides, Turkey. Sedimentary Geology, **181**(1-2):
538 39-57.

539 Knight, I., and James, N.P. 1987. The stratigraphy of the Lower Ordovician St. George
540 Group, western Newfoundland; the interaction between eustasy and tectonics.
541 Canadian Journal of Earth Sciences, **24**(10): 1927-1951.
542 Knight, I., James, N.P., and Lane, T.E. 1991. The Ordovician St. George unconformity,
543 Northern Appalachians; the relationship of plate convergence at the St. Lawrence
544 Promontory to the Sauk/Tippecanoe Sequence boundary. GSA Bulletin, **103**(9):
545 1200-1225.
546 Knight, I., Azmy, K., Boyce, W.D., and Lavoie, D. 2008. Tremadocian carbonate rocks
547 of the lower St. George group, Port au Port peninsula, western Newfoundland:
548 Lithostratigraphic setting of diagenetic, isotopic and geochemical studies. Current
549 Research, Newfoundland and Labrador Department of Natural Resources, **Report**
550 **08-1**: 115-149.
551 Land, L.S. 1983. The application of stable isotopes to studies of the origin of dolomite
552 and to problems of diagenesis of clastic sediments. *In* SEPM (Society for
553 Sedimentary Geology) Short Course Notes. *Edited by* M.A. Arthur, T.F.
554 Anderson, I.R. Kaplan, J. Veizer, and L.S. Land. pp. 4.1-4.22.
555 Land, L.S. 1992. The dolomite problem; stable and radiogenic isotope clues. *In* Lecture
556 Notes in Earth Sciences. *Edited by* N. Clauer and S. Chaudhure. pp. 49-68.
557 Lane, T.E. 1990. Dolomitization, brecciation and zinc mineralization and their
558 paragenetic stratigraphic and structural relationships in the upper St. George
559 Group (Ordovician) at Daniel's Harbour, western Newfoundland, Unpublished
560 PhD Thesis, Memorial University of Newfoundland, St. John's, Nfld.
561 Lavoie, D., Chi, G., Brennan-Alpert, P., Desrochers, A., and Bertrand, R. 2005.
562 Hydrothermal dolomitization in the Lower Ordovician Romaine Formation of the
563 Anticosti Basin: significance for hydrocarbon exploration. Bulletin of Canadian
564 Petroleum Geology, **53**(4): 454-471.
565 Lavoie, D., and Chi, G. 2006. Hydrothermal dolomitization in the Lower Silurian La
566 Vieille Formation in northern New Brunswick: geological context and
567 significance for hydrocarbon exploration. Bulletin of Canadian Petroleum
568 Geology, **54**(4): 380-395.
569 Lavoie, D., and Chi, G., in press. Lower Paleozoic foreland basins in eastern Canada:
570 Tectono-thermal events recorded by faults, fluids and hydrothermal dolomites.
571 Bulletin of Canadian Petroleum Geology, **56.**
572 McArthur, J.M., 1994. Recent trends in strontium isotope stratigraphy. Terra Nova **6**,
573 331–358.
574 Montanez, I.P., and Read, J.F. 1992. Fluid-rock interaction history during stabilization of
575 early dolomites, upper Knox Group (Lower Ordovician), U.S. Appalachians.
576 Journal of Sedimentary Research, **62**(5): 753-778.
577 Nowlan, G.S., and Barnes, C.R. 1987. Thermal maturation of Paleozoic strata in eastern
578 Canada from conodont colour alteration index (CAI) data with implications for
579 burial history, tectonic evolution, hotspot tracks and mineral and hydrocarbon
580 potential. Geological Survey of Canada, Bulletin **367**.
581 Shepherd, T.J., Rankin, A.H., and Alderton, D.H.M. 1985. A practical guide to fluid
582 inclusions. Blackie, London.
583 Shields, G.A., Carden, G.A.F., Veizer, J., Meidla, T., Rong, J., and Li, R.-Y. 2003. Sr, C,
584 and O isotope geochemistry of Ordovician brachiopods; a major isotopic event

around the Middle-Late Ordovician transition. Geochimica et Cosmochimica Acta, **67**(11): 2005-2025.

Smith, L.B., Jr. 2006. Origin and reservoir characteristics of Upper Ordovician Trenton-Black River hydrothermal dolomite reservoirs in New York. AAPG Bulletin, **90**(11): 1691-1718.

Smith, L.B., and Davies, G.R., 2006. Structurally controlled hydrothermal alteration of carbonate reservoirs: Introduction. AAPG Bulletin, **90**(11): 1635-1640.

Sperber, C.M., Wilkinson, B.H., and Peacor, D.R. 1984. Rock composition, dolomite stoichiometry, and rock/water reactions in dolomitic carbonate rocks. Journal of Geology, **92**(6): 609-622.

Stenzel, S.R., Knight, I., and James, N.P. 1990. Carbonate platform to foreland basin; revised stratigraphy of the Table Head Group (Middle Ordovician), western Newfoundland. Canadian Journal of Earth Sciences, **27**(1): 14-26.

Tucker, M.E., and Wright, V.P. 1990. Carbonate Sedimentology. Blackwell Publishing, Oxford, UK.

van Staal, C.R. 2005. North America; Northern Appalachians. *Edited by* R.C. Selley, L.R.M. Cocks, and I.R. Plimer Elsevier Academic Press, Oxford. pp. 81-92.

Veizer, J., Ala, D., Azmy, K., Bruckschen, P., Buhl, D., Bruhn, F., Carden, G.A.F., Diener, A., Ebneth, S., Godderis, Y., Jasper, T., Korte, C., Pawellek, F., Podlaha, O.G., and Strauss, H. 1999. $^{87}Sr/^{86}Sr$, $\delta^{13}C$ and $\delta^{18}O$ evolution of Phanerozoic seawater. Chemical Geology, **161**(1-3): 59-88.

Warren, J. 2000. Dolomite; occurrence, evolution and economically important associations. Earth-Science Reviews, **52**(1-3): 1-81.

Waldron, J.W.F., and van Staal, C.R. 2001. Taconian orogeny and the accretion of the Dashwoods block: A peri-Laurentian microcontinent in the Iapetus Ocean. Geology, **29**(9): 811-814.

White, D.E., 1957. Thermal waters of volcanic origin. Geological Society of America Bulletin, **68**: 1637-1658.

Wierzbicki, R., Dravis, J.J., Al-Aasm, I., and Harland, N. 2006. Burial dolomitization and dissolution of Upper Jurassic Abenaki platform carbonates, Deep Panuke reservoir, Nova Scotia, Canada. AAPG Bulletin, **90**(11): 1843-1861.

Williams, H. 1979. Appalachian Orogen in Canada. Canadian Journal of Earth Sciences, **16**(3, Part 2): 792-807.

Williams, S.H., Burden, E.T., and Mukhopadhyay, P.K. 1998. Thermal maturity and burial history of Paleozoic rocks in western Newfoundland. Canadian Journal of Earth Sciences, **35**(11): 1307-1322.

Figure Captions

Figure 1: Geological map of the Port au Port peninsula showing locating of the Isthmus Bay section (modified from Knight *et al.* 2008).

Figure 2: Simplified lithotratigraphy of the St. George Group, Port au Port peninsula with detailed section of the Watts Bight Formation showing the distribution of dolostones and limestones (adapted from Knight *et al.* 2008).

Figure 3: Photomicrographs of the Watts Bight Formation. (a) Stained thin section showing D1 dolomite replacing C1 micrite peloidal and intraclasts; (b) Photomicrograph of D2a and D2 dolomite; (c) Stained thin section showing Fe-poor (pink) and Fe-rich (purple) C3 infilling pores between D2b rhombs; (d) Stained thin section with D2b rhombs showing dissolution (dedolomitization) and infilling with Fe-rich C3 calcite; (e) D2b dolomite; (f) Same view as (a) under cathodoluminescence showing zoned orange/red luminescence of D2 dolomite and yellow fluorescence of C3 infilling pores.

Figure 4: Photomicrographs showing distribution of fluid inclusions. (a) Biphase inclusions in D2 dolomite rhomb. Note inclusion is elongate in the direction of growth of the dolomite rhomb. (b) Large biphase inclusion in C3 calcite. Microfractures around edge of inclusion may indicate leaking of trapped fluid.

Figure 5: Histogram of homogenization temperatures for fluid inclusions in the D2 and D3 dolomites and C3 calcite of the Watts Bight Formation.

Figure 6: Bivariate plot of homogenization temperature vs. salinity for fluid inclusions in the D2 and D3 dolomites and C3 calcite of the Watts Bight Formation.

Figure 7: Oxygen vs. Carbon isotope values for dolomite (D1, D2a, D2b, D3) and calcite (C1, C3). The square represents isotopic values for best preserved carbonate precipitated from Tremadoc seawater (Shields *et al.* 2003).

Figure 8: Scatter diagram showing the $^{87}Sr/^{86}Sr$ values in the Watts Bight dolomites (D1 to D3). The shaded area represents the range of $^{87}Sr/^{86}Sr$ values for the Tremadoc (Veizer *et al.* 1999; Shields *et al.* 2003)

Figure 9: Temperature vs. $\delta^{18}O_{fluid}$ for various $\delta^{18}O_{dolomite}$ derived from the fractionation equation: $10^3 \ln\alpha_{\text{dolomite-water}} = 3.2 \times 10^6 T^{-2} - 3.3$ (Lands, 1983). Hatched areas represent range of temperatures and $\delta^{18}O$ for various dolomite generations (D1, D2, D3). Values for Tremadoc seawater from Shields *et al.* (2003). See text for details.

Table 1: Fluid inclusion microthermometric data from the Watts Bight Formation

Phase		T_i	T_m (hydrohalite)	T_m(ice)	Salinity (eq. wt% NaCl)	X_{NaCl}	T_h (L)
D2	*n*	11	7	31	31	7	58
	Mean	-53.3	-34.6	-14.3	17.5	0.22	79.7
	Max.	-51.3	-31.9	-6.2	25.6	0.28	108.6
	Min.	-55.2	-39.1	-25.0	9.5	0.14	44.6
	S.D.	1.4	2.9	5.2	4.5	0.06	13.4
D3	*n*	3	4	8	8	3	7
	Mean	-51.1	-31.1	-16.9	20.1	0.31	114.0
	Max.	-50.2	-30.2	-14.7	23.2	0.34	130.1
	Min.	-52.0	-31.5	-21.3	18.4	0.29	91.4
	S.D.	0.9	0.6	2.2	1.6	0.03	13.3
C2	*n*	8	11	15	15	11	28
	Mean	-53.3	-30.9	-16.4	19.7	0.32	94.1
	Max.	-51.0	-26.1	-14.7	22.4	0.54	126.7
	Min.	-55.2	-34.6	-20.1	18.4	0.22	68.0
	S.D.	1.7	2.5	1.7	1.3	0.10	17.3

T_i = temperature of first ice melting; T_m(hydrohalite) = temperature of hydrohalite melting; T_m(ice) = temperature of last ice melting; X_{NaCl} = NaCl/ (NaCl + $CaCl_2$); T_h (L) = homogenisation temperature (to the liquid phase)

Table 2: Ca, Mg, Sr, Fe, Mn, $\delta^{13}C$ and $\delta^{18}O$ data for the Watts Bight Formation

Phase		$CaCO_3$ (%)	$MgCO_3$ (%)	Sr (ppm)	Fe (ppm)	Mn (ppm)	$\delta^{13}C$	$\delta^{18}O$
C1/C2	*n*	7	7	7	7	7	12	12
	Mean	98.5	1.5	320	168	64	-1.3	-7.8
	Max.	99.2	3.0	390	320	99	-0.3	-7.4
	Min.	97.0	0.8	239	95	35	-2.2	-8.4
	S.D.	0.8	0.8	50	82	23	0.6	0.3
C3	*n*	3	3	3	3	3	4	4
	Mean	99.0	1.0	155	155	31	-2.5	-7.7
	Max.	99.4	1.2	192	403	37	-1.5	-7.0
	Min.	98.8	0.6	101	21	24	-5.1	-8.5
	S.D.	0.3	0.3	48	215	6	1.7	0.7
D1	*n*	1	1	1	1	1	2	2
	Mean	64.1	35.9	257	1323	96	-1.0	-5.9
	Max.						-1.0	-5.5
	Min.						-1.0	-6.3
	S.D.						0.0	0.5
D2a	*n*	8	8	8	8	8	14	14
	Mean	58.3	41.7	79	765	63	-1.3	-9.2
	Max.	62.2	45.6	225	1242	82	-0.6	-6.0
	Min.	54.4	37.8	27	411	45	-1.8	-11.4
	S.D.	3.2	3.2	70	249	14	0.3	1.8
D2b	*n*	10	10	10	10	10	12	12
	Mean	60.0	40.0	112	537	69	-1.4	-8.2
	Max.	63.7	45.8	183	1126	114	-1.0	-5.5
	Min.	54.2	36.3	32	201	43	-1.9	-11.4
	S.D.	3.0	3.0	58	258	21	0.3	2.0
D3	*n*	1	1	1	1	1	3	3
	Mean	58.0	42.0	89	357	59	-1.4	-7.9
	Max.						-1.0	-5.6
	Min.						-2.1	-9.6
	S.D.						0.6	2.1

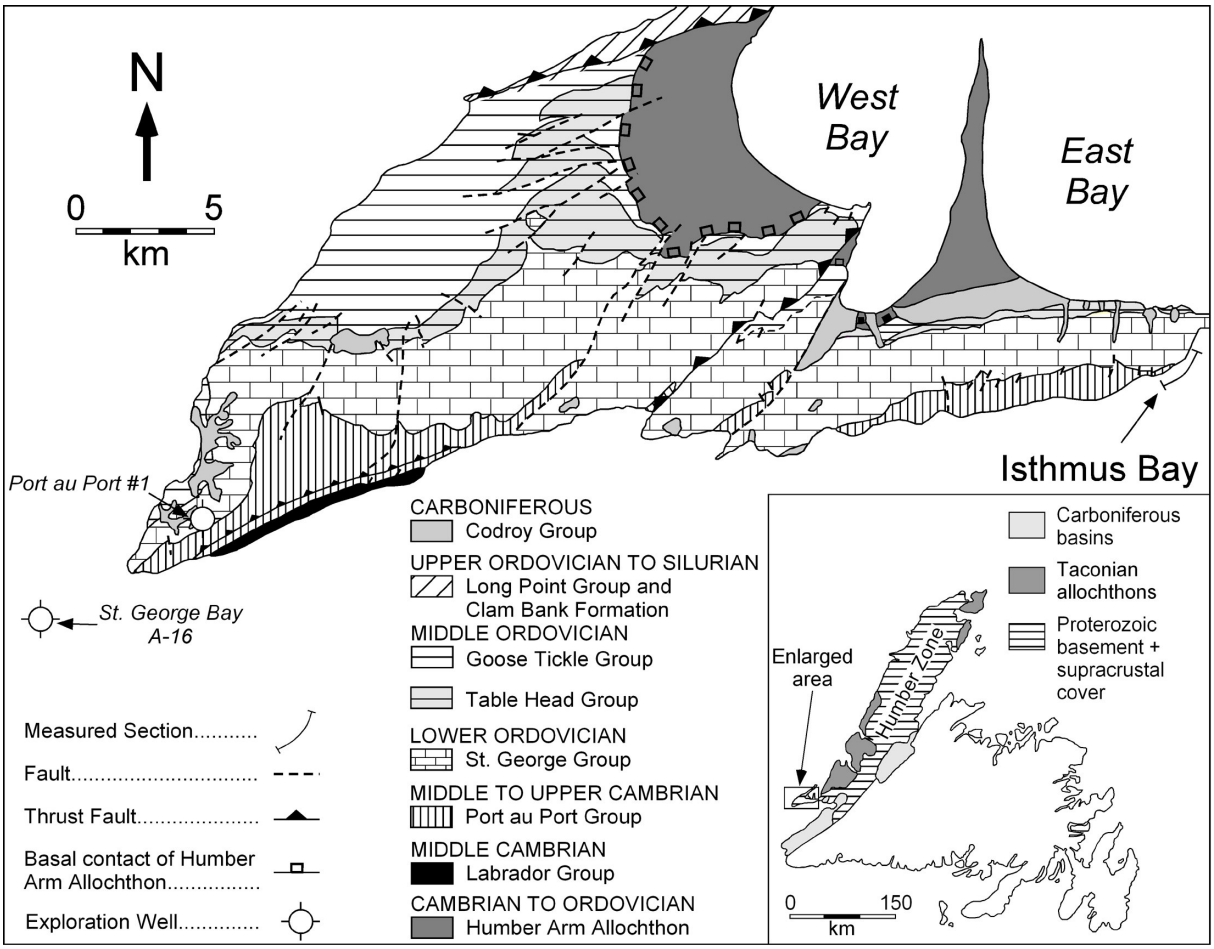
N
0
5
km
West Bay
East Bay
Isthmus Bay
Port au Port #1
St. George Bay A-16
CARBONIFEROUS
Codroy Group
UPPER ORDOVICIAN TO SILURIAN
Long Point Group and Clam Bank Formation
MIDDLE ORDOVICIAN
Goose Tickle Group
Table Head Group
LOWER ORDOVICIAN
St. George Group
MIDDLE TO UPPER CAMBRIAN
Port au Port Group
MIDDLE CAMBRIAN
Labrador Group
CAMBRIAN TO ORDOVICIAN
Humber Arm Allochthon
Measured Section.....
Fault.....
Thrust Fault.....
Basal contact of Humber Arm Allochthon.....
Exploration Well.....
Carboniferous basins
Taconian allochthons
Proterozoic basement + supracrustal cover
Enlarged area
Humber Zone
0
150
km

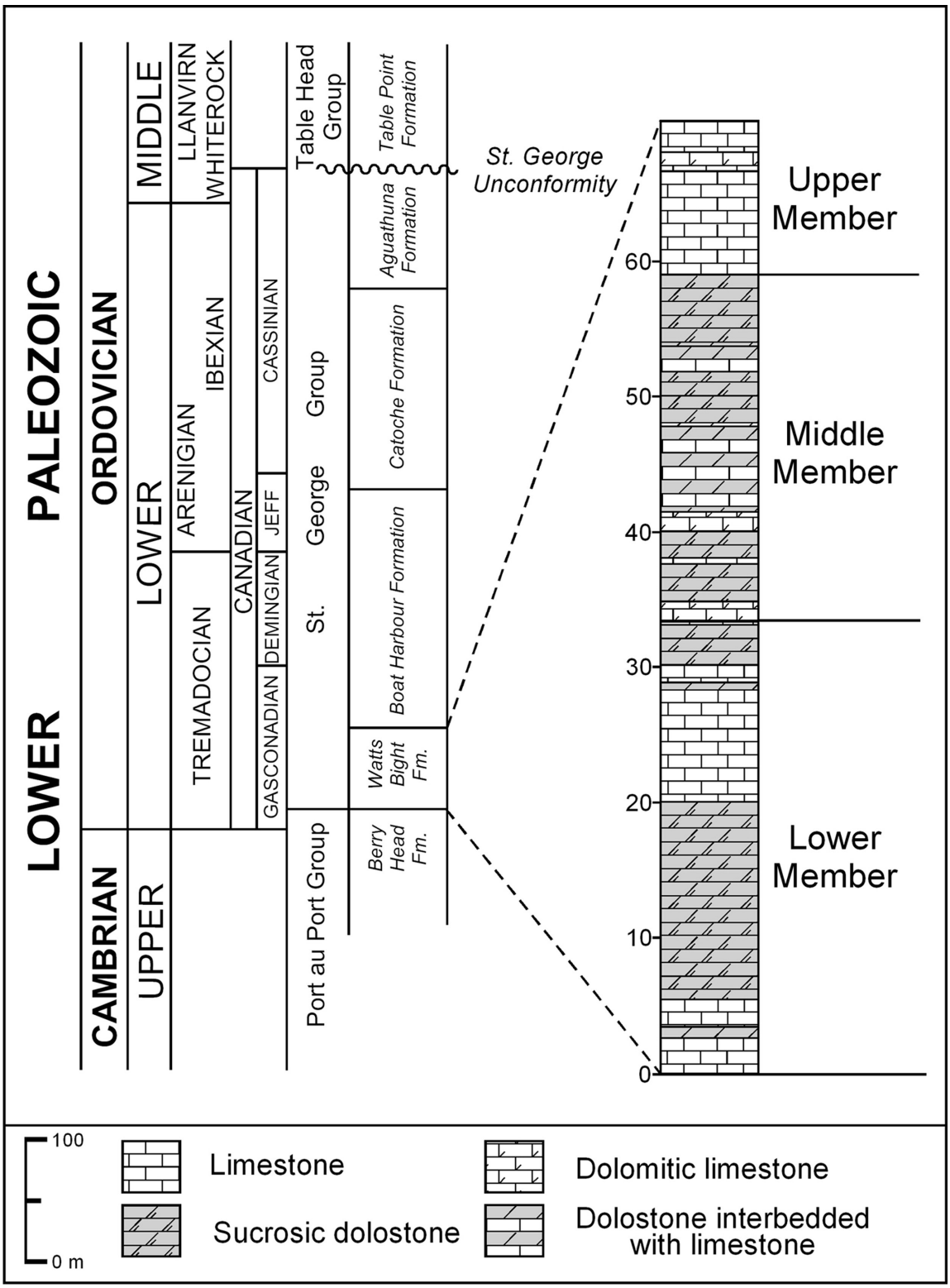
PALEOZOIC
LOWER
CAMBRIAN
UPPER
ORDOVICIAN
LOWER
MIDDLE
TREMADOCIAN
ARENIGIAN
LLANVIRN
WHITEROCK
IBEXIAN
CANADIAN
GASCONADIAN
DEMINGIAN
JEFF
CASSINIAN
Port au Port Group
St. George Group
Table Head Group
Berry Head Fm.
Watts Bight Fm.
Boat Harbour Formation
Catoche Formation
Aguathuna Formation
Table Point Formation
St. George Unconformity
Upper Member
Middle Member
Lower Member
60
50
40
30
20
10
0
100
0 m
Limestone
Sucrosic dolostone
Dolomitic limestone
Dolostone interbedded with limestone

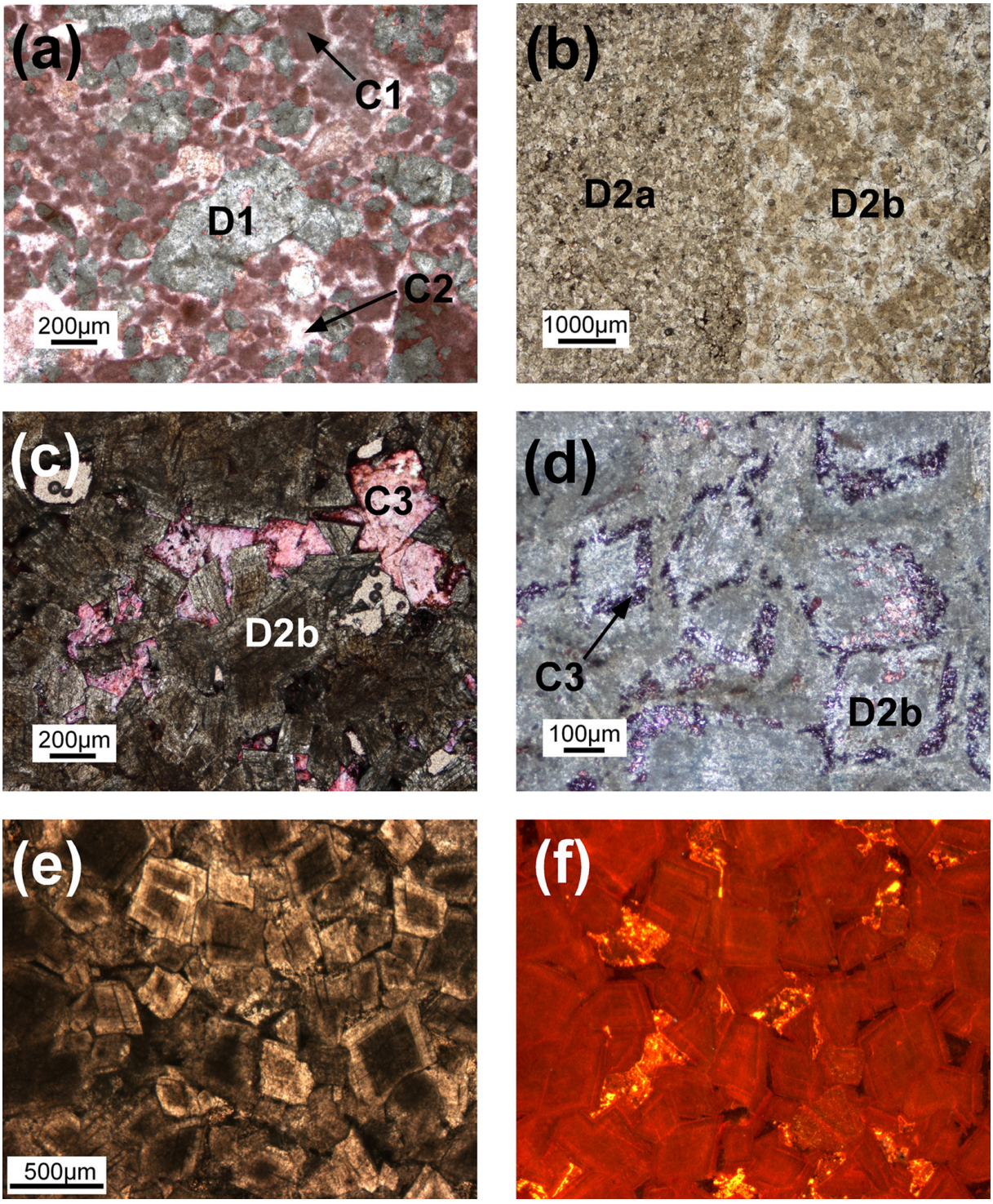
(a)
C1
D1
C2
200μm
(b)
D2a
D2b
1000μm
(c)
C3
D2b
200μm
(d)
C3
D2b
100μm
(e)
500μm
(f)

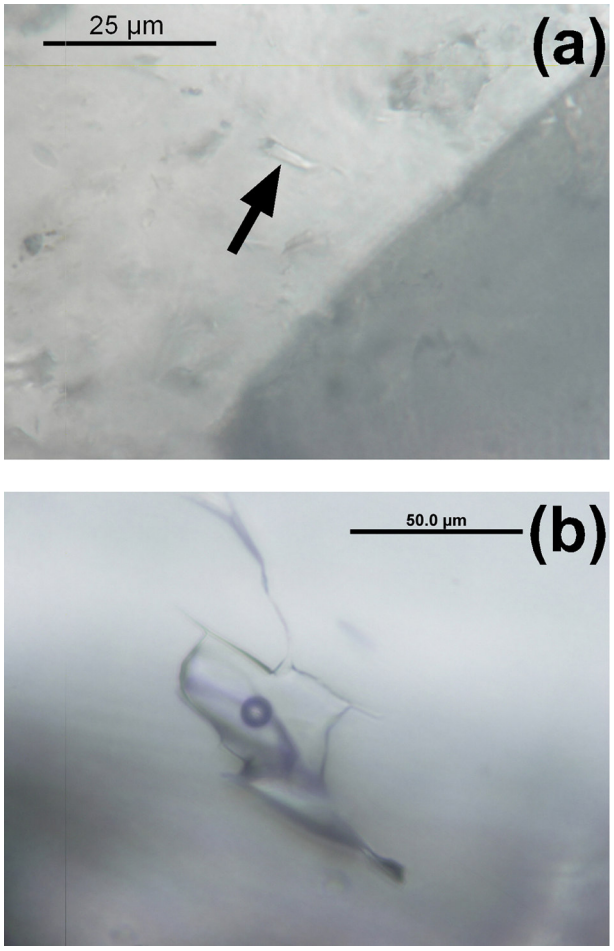
25 µm
(a)
50.0 µm
(b)

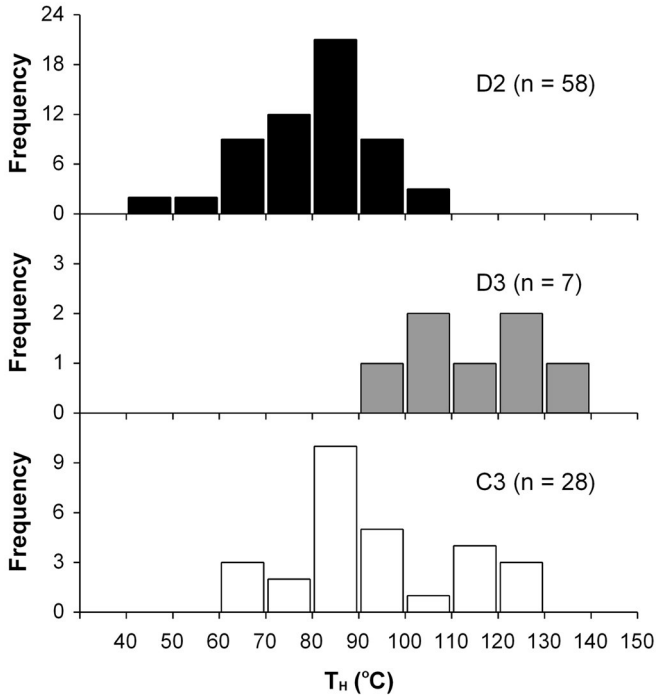
Frequency
24
18
12
6
0
D2 (n = 58)
Frequency
3
2
1
0
D3 (n = 7)
Frequency
9
6
3
0
C3 (n = 28)
40 50 60 70 80 90 100 110 120 130 140 150
T_H (°C)

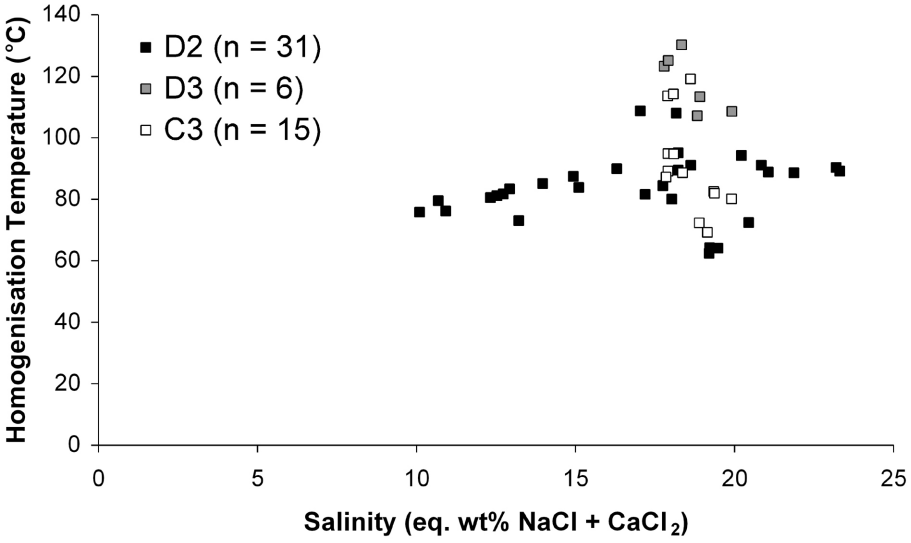
D2 (n = 31)
D3 (n = 6)
C3 (n = 15)
Homogenisation Temperature (°C)
Salinity (eq. wt% NaCl + CaCl2)
0
20
40
60
80
100
120
140
0
5
10
15
20
25

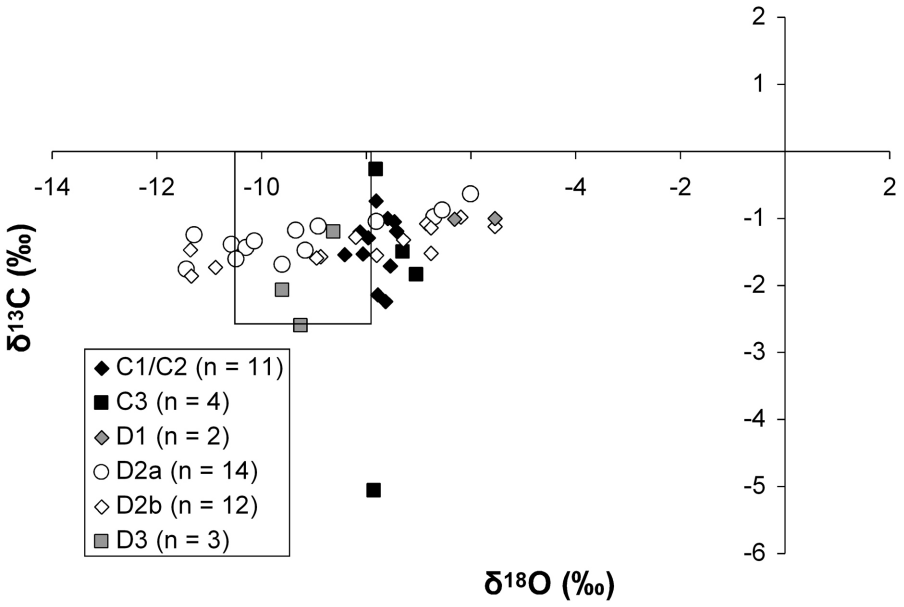
2
1
-14
-12
-10
-4
-2
2
-1
-2
-3
-4
-5
-6
δ13C (‰)
δ18O (‰)
C1/C2 (n = 11)
C3 (n = 4)
D1 (n = 2)
D2a (n = 14)
D2b (n = 12)
D3 (n = 3)

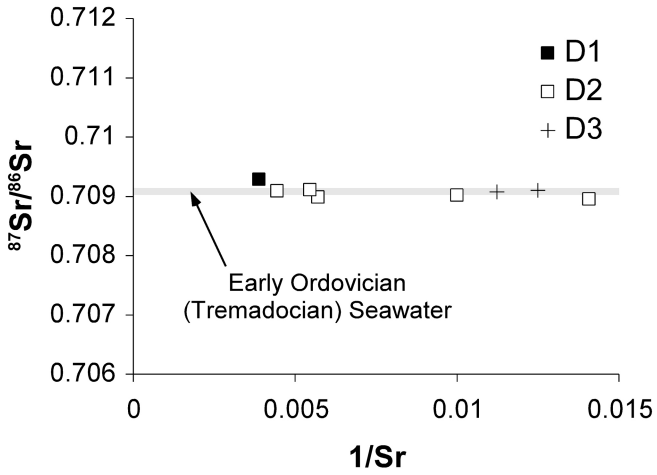
0.712
0.711
0.71
0.709
0.708
0.707
0.706
$^{87}Sr/^{86}Sr$
0
0.005
0.01
0.015
1/Sr
D1
D2
D3
Early Ordovician
(Tremadocian) Seawater

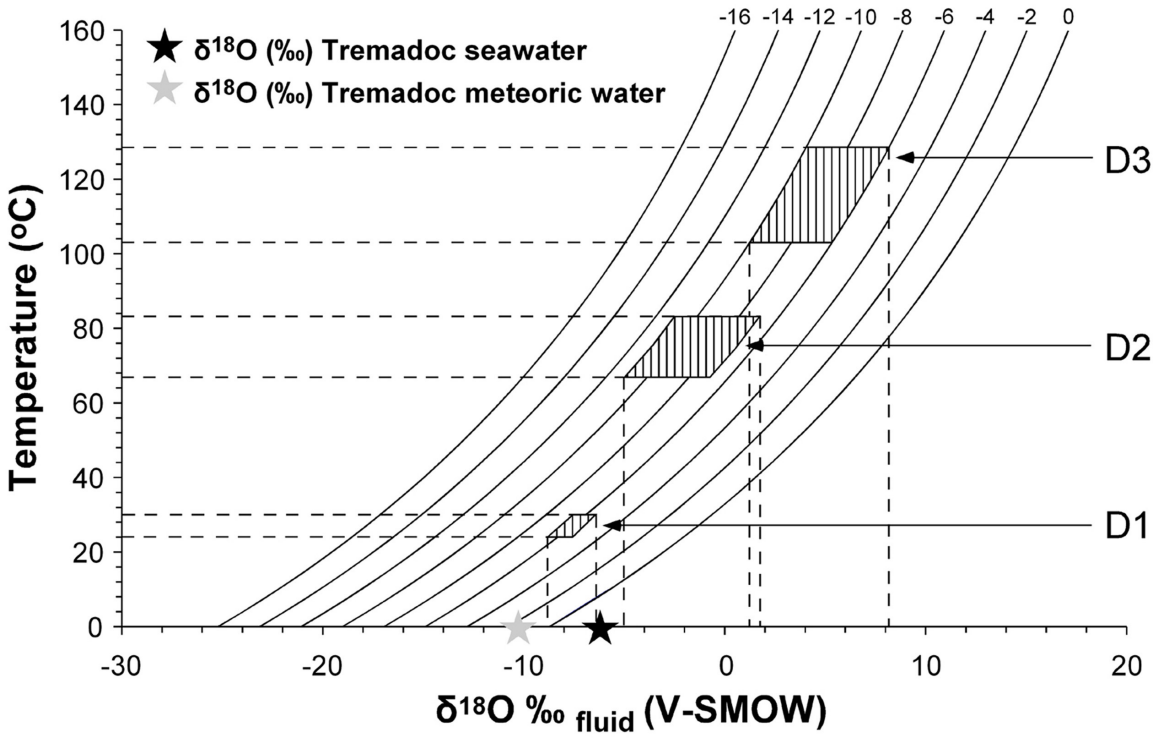
-16 -14 -12 -10 -8 -6 -4 -2 0
δ18O (‰) Tremadoc seawater
δ18O (‰) Tremadoc meteoric water
D3
D2
D1
Temperature (°C)
160
140
120
100
80
60
40
20
0
-30
-20
-10
0
10
20
δ18O ‰ fluid (V-SMOW)

Appendix A. Samples, description, elemental and isotopic compositions, visual porosity estimates and permeability in the Watts Bight Formation.

Sample ID	Phase	Formation	Depth (m)	$CaCO_3$ (%)	$MgCO_3$ (%)	Sr (ppm)	Mn (ppm)	Fe (ppm)	$\delta^{18}O$ (‰ VPDB)	$\delta^{13}C$ (‰ VPDB)	$^{87}Sr/^{86}Sr$	Visual estimate of porosity (%)	Permeability (mD)
WB30	C1/C2	Watts Bight	68	98.50	1.50	239	70	320	-8.41	-1.54		<1	
WB26	C1/C2	Watts Bight	60	99.07	0.93	390	35	128	-8.06	-1.53		0	
WB22	D2a	Watts Bight	58.3	54.37	45.63	32	75	1242	-11.43	-1.76		4	
	D2b	Watts Bight		54.20	45.80	32	74	1126	-11.34	-1.86			1.30
WB21	D2b	Watts Bight	56.8						-7.80	-1.55		<1	
WB24	D3	Watts Bight	55.9	57.97	42.03	89	59	357	-9.60	-2.07	0.709075	1	
WB21	D2a	Watts Bight	54.8						-9.60	-1.69			
WB20	C3	Watts Bight	53.9	98.78	1.22	173	24	21	-7.85	-5.06		0	
WB18	D2a	Watts Bight	50.4	54.82	45.18	41	67	744	-9.16	-1.48		4	1.42
WB17	D2b	Watts Bight	48.1									4	1.28
WB16	D2a	Watts Bight	45.8						-10.48	-1.61		<1	
WB15	C1/C2	Watts Bight	43.5	97.02	2.98	275	99	228	-7.63	-2.24		0	
	D2a	Watts Bight		62.19	37.81	59	52	773	-10.29	-1.44		<1	
WB14	D2a	Watts Bight	42						-6.70	-0.98		<1	
WB13	D2a	Watts Bight	40.2						-8.91	-1.12		0	
WB12	C1/C2	Watts Bight	37.9						-7.78	-2.14		<1	
WB11	D2b	Watts Bight	35.6	57.30	42.70	100	60	326	-8.20	-1.28	0.709015	1	
	D3	Watts Bight							-8.62	-1.20	0.7091		
WB10	D1	Watts Bight	33.6	64.10	35.90	257	96	1323	-6.31	-1.01	0.709283	0	
WB9	D2b	Watts Bight	31.7	60.65	39.35	171	68	586	-6.85	-1.08	0.708953	1	
WB8	C1/C2	Watts Bight	29.8	98.41	1.59	335	81	182	-7.96	-1.29		<1	
WB-7	C3	Watts Bight	27.4	98.94	1.06	101	33	41	-7.30	-1.50		<1	
	D2a	Watts Bight							-6.54	-0.88			
WB6	C1/C2	Watts Bight	25.1	99.18	0.82	346	74	114	-7.81	-0.27		<1	
	C1/C2	Watts Bight							-7.81	-0.74			

Appendix A *(continued)*

Sample ID	Phase	Formation	Depth (m)	$CaCO_3$ (%)	$MgCO_3$ (%)	Sr (ppm)	Mn (ppm)	Fe (ppm)	$\delta^{18}O$ (‰ VPDB)	$\delta^{13}C$ (‰ VPDB)	$^{87}Sr/^{86}Sr$	Visual estimate of porosity (%)	Permeability (mD)
WB5	D2a	Watts Bight	22.7	60.24	39.76	27	50	411	-11.28	-1.25		3	
WB4	C1/C2	Watts Bight	21.2	99.15	0.85	341	42	108	-7.59	-1.00		1	
WB3	D2b	Watts Bight	18.3						-9.34	-1.18		7	16.50
WB2	D2b	Watts Bight	15.9	62.81	37.19	121	54	492	-7.29	-1.32		3	
WB1	D2a	Watts Bight	14.6	55.25	44.75	38	54	554	-10.57	-1.39		4	
	D2b	Watts Bight		60.81	39.19	32	54	460	-10.88	-1.73			
WBA1	D2b	Watts Bight	13.3						-8.87	-1.57		7	1.95
WBA2	D2b	Watts Bight	11.7									7	10.05
WBA3	D2b	Watts Bight	10						-6.84	-2.29		2	1.90
WBA4	D2a	Watts Bight	8	62.07	37.93	225	82	940	-6.00	-0.64	0.70909	<1	
	D2b	Watts Bight		60.41	39.59	183	61	423	-5.54	-1.12	0.709106		
WBA5	D2a	Watts Bight	5.9	59.78	40.22	142	45	694	-7.80	-1.05		<1	
	D2b	Watts Bight		63.72	36.28	134	43	386	-6.76	-1.14			
WBA6	C1/C2	Watts Bight	4.5	98.30	1.70	313	50	95	-7.42	-1.19		<1	
	D2a	Watts Bight		57.36	42.64	64	77	759	-10.13	-1.34			
	D2b	Watts Bight		57.84	42.16	48	91	633	-11.36	-1.47		5	
	D3	Watts Bight							-5.57	-0.99			
WBA7	C1/C2	Watts Bight	0.9						-7.54	-1.71		<1	
	C1/C2	Watts Bight							-8.12	-1.20			
	C3	Watts Bight		99.39	0.61	192	37	403	-7.04	-1.84			
WBA8	C1/C2	Berry Head	0						-7.46	-1.05		<1	
	D2b	Berry Head		63.67	36.33	175	69	201	-6.19	-0.98	0.708984		
WBA9	D2b	Berry Head	-1.6	52.45	47.55	43	49	424	-8.95	-1.59		4	2.00
WBA10	D1	Berry Head	-3.7						-5.54	-1.00		<1	
WBA11	D2b	Berry Head	-5.2	59.03	40.97	120	114	736	-6.76	-1.52		2	